

Journal of Rehabilitation in Civil Engineering

Journal homepage: https://civiljournal.semnan.ac.ir/

Investigate the Mechanical Characteristics and Microstructure of Fibrous-Geopolymer Concrete Exposure to High Temperatures

Arjan Fakhrulddin Abdullah ^{1*}; Mazin Burhan Al-Deen Abdul-Rahman ²; Alyaa Abbas Al-Attar ²

- 1. Department of Civil Engineering, Structure Engineering, Faculty of Engineering, Tikrit University, Iraq
- 2. Department of Civil Engineering, Building Constriction Material, Northern Technical University, Iraq
- * Corresponding author: arjan.fakhruldeen@st.tu.edu.iq

ARTICLE INFO

Article history: Received: 28 July 2024 Revised: 13 November 2024

Accepted: 15 January 2025

Keywords: Geopolymer concrete; Fire exposure; Alkaline activation; Steel fiber.

ABSTRACT

The main objective of this study is to evaluate the mechanical properties of geopolymer concrete (GPC), made from alkalineactivated fly ash and Ground Granulated Blast Furnace Slag (GGBS), compared to conventional M30 grade concrete. Additional samples of GPC incorporating steel fibers were also tested. To investigate the behavior of these materials under elevated temperatures (0°C, 250°C, 500°C, 750°C), specimens were cast and tested, including cubes, cylinders, and prisms. These specimens comprised slag-based GPC (containing GGBS and fly ash) and standard M30 concrete. The results of the compressive strength tests indicated that GPC demonstrated 22.3% greater strength than conventional concrete. Furthermore, adding steel fibers to GPC enhanced its compressive strength by 61%. The split tensile strength of GPC was 71.8% higher than standard concrete, and GPC with steel fibers exhibited a 118.5% increase. Similarly, the flexural strength (modulus of rupture) increased by 22% for GPC and 54% for GPC reinforced with steel fibers, compared to conventional concrete. Overall, the findings reveal that incorporating steel fibers significantly improves the of mechanical properties slag-based GPC, particularly in compressive, tensile, and flexural strength, making it superior to ordinary Portland cement (OPC)-based concrete.

E-ISSN: 2345-4423

© 2025 The Authors. Journal of Rehabilitation in Civil Engineering published by Semnan University Press. This is an open-access article under the CC-BY 4.0 license. (https://creativecommons.org/licenses/by/4.0/)

How to cite this article:

Abdullah, A. Fakhrulddin, Abdul-Rahman, M. Burhan Al-Deen and Al-Attar, A. Abbas (2026). Investigate the Mechanical Characteristics and Microstructure of Fibrous-Geopolymer Concrete Exposure to High Temperatures. Journal of Rehabilitation in Civil Engineering, 14(1), 2141 https://doi.org/10.22075/jrce.2025.34716.2141

1. Introduction

Despite being the dominant construction material for many years, concrete is encountering difficulties in satisfying the demand for environmentally friendly and sustainable building materials [1–8]. Many scientists actively explore novel environmentally sustainable materials [9,10]. A growing trend involves replacing cement with low-energy materials or construction waste [11–13].

GPC offers outstanding mechanical properties and resistance to high temperatures, fire, alkalis, and acids [14,15]. As a sustainable alternative to traditional cement, it reduces carbon emissions, making it crucial for environmentally friendly construction practices [16–18]. The polymerization process in GPC involves activating aluminosilicate materials using various activators, resulting in different geopolymers: acid-activated, alkali-activated, and salt-activated. This process results in a rapid-curing material with superior strength, excellent thermal stability, and durability, making GPC highly suitable for use in building materials, especially in applications requiring resilience to high temperatures and harsh environments [18,19].

With the ongoing advancement of contemporary urbanization and the subsequent rise in building density, ensuring the fire resistance of structures has become a crucial and pressing issue. Several parts of a structure may be damaged to various extents throughout a fire. They may even be at risk of collapsing, a significant danger to people's lives and property. Thus, it is essential to guarantee fire resistance of buildings throughout the construction of various civil structures and infrastructures. Studies [20,21] show that GPC has illustrated outstanding resilience to high temperatures.

Additionally, Razak et al. [22] found that GPC exhibited improved mechanical strength and a more compact structure when exposed to 500 °C. Consequently, GPC demonstrated greater structural integrity and thermal stability than normal concrete. Türkmen et al. [23] examined the water absorption and fire resistance characteristics of GPC using two distinct aggregate types (crushed sand aggregate and river sand aggregate). They found that the water absorption increased at 700 °C, while the compressive strength of the GPC specimens increased at temperatures of 100 and 300 °C. In recent studies, researchers have extensively investigated the various factors that influence the elevated temperature characteristics of GPC. They have found that factors such as conservation conditions, exposure time, exposure temperature, heating rate, and cooling method all influence the mechanical properties of GPC after exposure to high temperatures.

Yazdi et al. [24] investigated the relationship between the mechanical characteristics and microstructural of geopolymers made from slag and fly ash at normal temperature using various proportions of FA were replaced with GGBS to improve the initial geopolymers strength development healed at the normal temperature. Compressive and flexural strength tests have been performed to measure mechanical features; the flexural and compressive strengths of geopolymers with slag reached 100 and 10 MPa, accordingly. The reduction in geopolymers' porosity corresponded with the increasing compressive strength magnitudes. Nevertheless, despite an increase in flexural strength, neither improved significantly when more than half of the FA was replaced by GGBS.

He et al. [25] reviewed the mechanical and thermal characteristics of geopolymers exposed to high temperatures. They concluded that geopolymers have excellent thermal stability at extreme temperatures and that the proportion of expansion, loss of mass, and thermal conductivity of burned geopolymers are much lower than those of OPC. They also concluded that composition has a lower influence on geopolymer failure behavior under thermal conditions than strength.

Korniejenko et al. [26] examined the geopolymer mechanical characteristics dependent on fly ash strengthened with short natural fibers from plants like coconut, raffia, cotton, and sisal. This research explores the impact of adding various natural fibers on the geopolymer mechanical characteristics. The

findings show that the suitable incorporation of natural fibers can improve the mechanical properties of geopolymer composites.

Cheng et al. [27] investigated the effects of textile sludge substituting aggregates and cement on polypropylene fiber concrete compressive strength, heavy metal leaching concentration, micromorphology, drying shrinkage, and nano-mechanical characteristics. The outcomes indicate that the concrete containing textile sludge effectively solidifies heavy metal ions. Using 10% textile sludge instead of cement enhances the concrete microstructure, increasing high-density calcium silicate hydrate production and reducing interfacial transition zone thickness.

Hai et al. [28] studied geopolymer mortar's thermal behavior and mechanical features after exposure to high temperatures. They describe the experimental test findings on the mechanical characteristics and thermal reaction of geopolymer mortar made from an alkaline solution activating a blend of fly ash and metakaolin. Extensive experiments were performed on geopolymer mortar, including bond strength, tensile, compressive, and bending tests. According to the findings, geopolymer mortar's bond strengths, tensile, compressive, and bending increase at 100 degrees centigrade and then decline in the 300-700 degree centigrade ranges. Furthermore, compared with regular Portland cement mortar, geopolymer mortar shows reduced temperature-induced degradation in compressive and bond strength but higher temperatureinduced degradation in bending and tensile strength. Sarker et al. [29] examined and contrasted nine mixes of Self-Compressed Geopolymer Concrete (SCGPC) before and after being exposed to fire as part of an experimental program. To illustrate the impact of 5 substitute proportions of slag and fly ash and 5 volumetric proportions of steel fibers on these qualities, they performed five new property tests and compared the material behavior. According to test findings, every designed SCGPC mix has flowability, filling capacity, and passing ability that aligns with the requirements. However, for a blend of 50 percent fly ash and 50 percent slag, the amount of steel fibers added should not exceed 0.75%. The tested SCGPC slabs exhibit good thermal conductivity, heat insulation, and fire resistance. SCGPC slabs show better residual flexural strength than SCC slabs in the post-fire test. This research used varied proportions of previously recycled materials, adding steel fibers to increase their strength. These mixes were then subjected to various temperatures to identify their mechanical features.

These days, the most prevalent sources of silicate minerals are fly ash, metakaolin, silica fume, and GGBS. Under the same conditions, GPC is superior to standard Portland cement concrete in tensile strength, durability, compressive strength, CO2 emissions, fire resistance, and setting time. The use of fiber-reinforced materials improves the GPC compressive strength. The fundamental reason for this phenomenon is that fiber has a more negligible influence than water-binder proportion, aggregate type, curing environment, and age. Factors such as the volume rate, shape, type, and aspect proportion of fiber in Ground Granulated Blast Furnace Slag fluence geopolymer concrete's splitting tensile strength and flexural strength. Steel fiber greatly enhances these characteristics. Hooked-end performance is superior at the same volume rate. However, the mechanical properties were evaluated at three different temperatures and compared with the original values before exposure. Furthermore, the results were compared to conventional concrete at the same temperature, which has the same compressive strength but employs ordinary cement. However, the current study considered the first one that explored the GPC microstructure under four temperatures (0, 250, 500, and 750) degrees centigrade.

The importance of this work lies in its contribution to the development of more resilient and sustainable construction materials. By investigating the mechanical characteristics and microstructure of fibrous-geopolymer concrete (GPC) under high-temperature exposure, this study provides valuable insights into the performance of GPC, which is made from eco-friendly materials such as fly ash and GGBS. The findings demonstrate that GPC outperforms conventional concrete in strength and that adding steel fibers further enhances its compressive, tensile, and flexural properties, particularly under extreme conditions like high temperatures. This research is crucial for advancing sustainable, high-performance materials in

infrastructure projects and promoting environmental conservation while improving structural durability and fire resistance.

2. Experimental Program

Figure 1 defines the experimental programs used in this work.

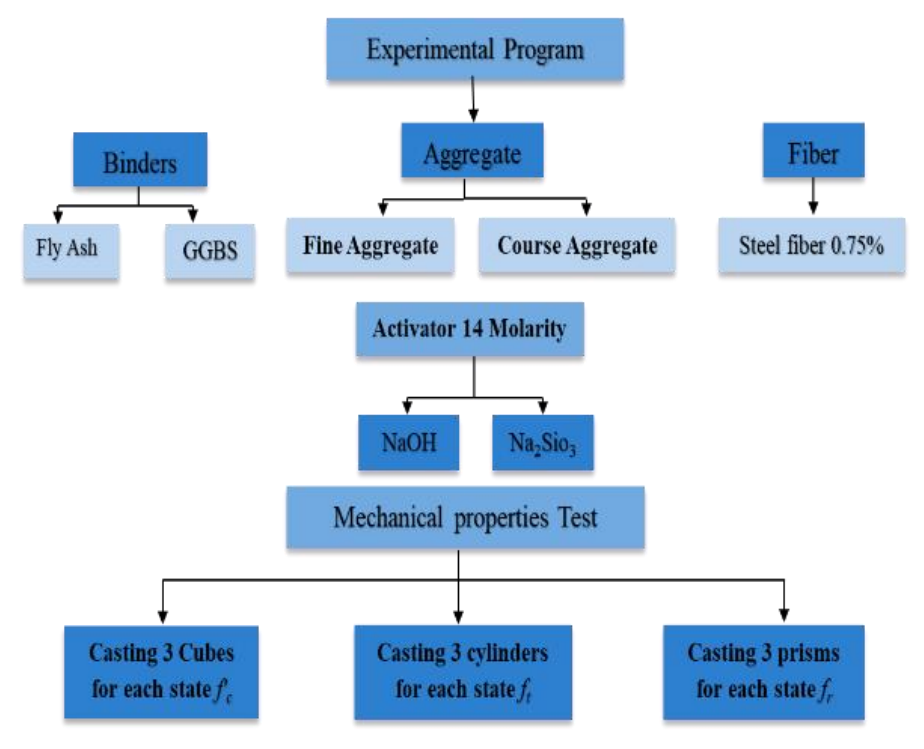


Fig. 1. The Experimental Work Program Flow Chart.

2.1. Materials

2.1.1. Fly Ash

Fly ash is a fine powder byproduct from pulverized coal combustion in electric generating stations. It consists primarily of calcium oxides, iron, aluminum, and silicon. Using fly ash in concrete can reduce the material's environmental footprint, as it reuses a waste product and reduces the amount of cement required. Table 1 indicates the characteristics of the materials utilized for the experiment study, and Table 2 illustrates the chemical composition and physical characteristics of fly ash.

2.1.2. Ground Granulated Blast Furnace Slag (GGBS)

A byproduct of the blast furnaces utilized to produce iron is called ground granulated blast furnace slag (GGBS). GGBS is widely utilized in the construction industry as a supplementary cementitious material. When mixed with Portland cement, it enhances the features of concrete, such as durability, workability, resistance to chemical attack, and sustainability. The characteristics of the materials utilized for the experiment study are indicated in Tables 1 and 2, which display the physical characteristics and chemical composition of GGBS.

2.1.3. Ordinary Portland Cement

This research utilizes ordinary Portland cement (class I), produced at the Almas Cement Factory in Iraq, to refer to normal concrete beam samples. Tables (2 and 3) demonstrate the cement's chemical analysis and physical test findings, respectively. The test findings indicated that the cement utilized conformed to Iraqi Requirement No. 5/1984 [30].

2.1.4. Alkaline-Activated Solution

The alkaline solution was mixed with sodium silicate (Na₂SiO₃) and sodium hydroxide (NaOH). The sodium hydroxide used was 97% pure and available in solid form commercially. The NaOH solution was prepared by dissolving the flakes or pellets in water. The amount of NaOH solids present in a solution is determined by the amount of the solution, which can be determined in molarity.

2.1.5. River Sand

This research utilized natural sand as the fine aggregate, and sieve analysis was conducted to determine the fineness modulus of the sand. Table 1 presents the chemical and physical characteristics of the fine aggregate, which meet the specifications given in the ASTM C33/C33M. The fine aggregate grading is presented in Table 4.

2.1.6. Coarse Aggregate

Small-sized coarse aggregate is used throughout this study. A pycnometer test was performed to identify the specific gravity of the aggregates. Sieve analysis was performed to find the fineness modulus of the aggregate. Table 1 displays the physical characteristics of the coarse aggregate. Dust and dirt were removed by washing the aggregate. The coarse aggregate grading is presented in Table 5.

2.1.7. Steel Fibers

The steel fibers utilized in this study are hook-end steel fibers, depicted in Figure 2. The high-tensile fibers possess a maximum tensile strength of up to 1345 MPa. They have a diameter of about 0.55 mm, a length of around 50 mm, and an aspect ratio of 91.



Fig. 2. Hook-end Steel Fibbers.

Table 1. Utilized materials characteristics.

No	Material	Specific Gravity	Specific surface area	Water Absorption %	Dry Loose Unit Weight kg/m3	Sulfate amount (As SO3) (%)	Material Finer than Sieve 0.075 mm
1	Cement (OPC) Type I	3.1	$300 \text{ m}^2/\text{kg}$	27.6	-	-	-
2	Fly Ash	2.41	$525 \text{ m}^2/\text{kg}$		-	-	-
3	GGBS slag	2.59	$293 \text{ m}^2/\text{kg}$		-	-	-
4	Coarse aggregate	2.68		1.15	1620	0.087	-
5	Fine aggregate	2.45		1.25	1793	0.073	1.85

Table 2. Oxide Composition of Cement, Fly Ash, and GGBS
--

Ovides commercial	Content (%)					
Oxides composition	Cement	FA	GGBFS			
CaO	58.29	1.58	30.1			
$\mathrm{Al_2O_3}$	4.61	22.13	8.77			
$ m SiO^2$	20.31	63.21	35.42			
Fe_2O_3	3.99	7.15	1.99			
MgO	3.5	2.39	6.93			
SO_3	2.04	0.11	0.43			
Loss of Ignition (L.O.I)	4.35	1.56	0.83			

^{*}The tests are conducted at the National Laboratory.

Table 3. Physical features of utilized cement*.

Physical features	Findings	Limit of (IQS No.5. /1984) [30]
Fineness (m ² /kg)	353	> (230)
Initial setting (min)	2hrs 25min	> (45)
Final setting (hour)	4hrs 10min	<(10)
Compressive strength 3 days (MPa)	18.3	>15 MPa
Compressive strength 7 days (MPa)	26.7	>23 MPa

Table 4. Results of grading of fine aggregate*.

		
Sieve Number	Passing (%)	Limit of IQS No. 45/1984 for zone No. (3)
4.75-mm (No.4)	99	90-100
2.36-mm (No.8)	87	85-100
1.18-mm (No.16)	79	75-100
600-μm (No.30)	32	60-79
300-μm (No.50)	26	12-40
150-μm (No.100)	1	0-10

Table 5. Results of grading of coarse aggregate*.

	<u> </u>	66 6
Sign (mm)	Passi	ing (%)
Size (mm)	Coarse Aggregate (%)	IQS No. 45/1984
14	100	(90-100)
10	73.4	(50-85)
5	3.3	(0-10)
PAN	0	-

3. Mix Design

3.1. Mix Design of Conventional Concrete (M30 Grade)

Table 6 illustrates normal concrete quantities for the current work. This mixture was designed using the American Concrete Institute method of mix design (ACI-211.1) to gain 30 MPa compressive strength, equivalent to GPC. It was intended to be compared with the GPC under various temperatures while maintaining the same compressive strength as normal concrete.

Table 6. Mix design of normal concrete.

		<u> </u>		
No	Cement (Kg/m ³)	Coarse aggregate (Kg/m ³)	Fine Aggregate (Kg/m ³)	Water (Kg/m ³)
1	355	980	775	195.6

3.2. Mix Design for Geopolymer-Based Concrete

The present research uses the processes commonly employed by researchers in the past to develop the mixture. In most GPC mixes, coarse and fine aggregates account for about 75 percent of the total mix mass.

This rate is similar to OPC concrete, which ranges from 75% to 80% of the concrete mix by amount. Fine aggregate was taken for half an hour for the whole mixture [31]. The typical density of fly ash and slag, mostly reliant on GPC, has been measured similarly to that of OPC concrete, which is 2400 kg/m3, as the literature review.supports The slag and fly ash amount and alkaline solution are identified by taking the proportion of Na₂SiO₃ solution to NaOH solution, utilizing the combined mass and the quantitative relation of (fly ash/slag) to alkaline liquid. The following criteria were maintained for various trial mixes supported by past work allotted [32].

- 1) The proportion of alkaline liquid to binder = 0.45
- 2) Proportion of Na_2SiO_3 to NaOH = 2.25
- 3) Molarity = M14
- 4) Temperature of Curing = 75° C
- 5) Time of Curing = 24 h
- 6) Rest Period = 1 day
- 7) Dosage of Admixtures = 2%.

Various variations and mixtures were performed, maintaining the given parameters constant and adjusting the proportion of fly ash to slag with various mixes to achieve a comparable compressive strength of M30 grade of control concrete. Tables 7 and 8 present the target mix design and the trail mix design process, respectively.

Table 7. Trail mix design for GPC.

Mix No.	cement	GGBS%	Fly ash%	f_{cu} 28day	f_{cr} 28day	f_t 28day
1	0	30	70	17.5	1.71	3.92
2	0	70	30	28.5	2.65	5.1
3	0	50	50	24.5	2.36	5.36
4	0	60	40	40.2	2.7	5.4
5	10	50	40	31.5	1.50	4.78

Mix No. 4 was selected as the initial mix for the successful GPC due to its ultimate compressive, splitting tensile, and flexural strengths observed over seven curing days. This mixture was approved and used to cast the remaining concrete models, as shown in Figure 3.



Fig. 3. Trail mix cubes for geopolymer mix.

	Table 6. Qualities for Green selected him design.									
Quantities m ³	Coarse aggregate Kg	Fine aggregate Kg	GGBS Kg	Fly Ash Kg	AA/Binder	HS/SS	NaOH Kg	Na ₂ SiO ₃ Kg	10% (Extra water+S.P)Kg	S.T Fiber 0.75%
1	1210	650	240	160	0.45	2.25	55.4	124.6	40	58.88

Table 8. Quantities for GPC for selected mix design.

4. Preparation, Mixing, Casting, and Curing of Concrete

4.1. Preparation of Alkaline Activator Solution

The alkaline activator solution (AAS) plays a vital role in the polymerization reaction of GPC. In this research, 14 molarity solutions were used dependent on various mortar compression tests to make (AAS); when water is mixed with NaOH, a percentage of heat is generated due to an exothermic reaction, as illustrated in (Figure 4a).

Na₂SiO₃ solution is commercially available in various grades; throughout this study, the Na₂SiO₃ solution had a 2.4 mass proportion of SiO₂ to Na₂O. To make (AAS), NaOH is produced as a solution and added to the Na₂SiO₃ solution (Figure 4b). In this research (AAS) was produced 24 hours before casting.



a) Mixing NaOH with water.



b) Final form of activator (AAS).

Fig. 4. Preparation of 14 M alkaline activator solution.

4.2. Mixing of Geopolymer Concrete

Materials used to cast the sample were first balanced in surface dry condition. All these components were combined for four to five minutes and kept dry on the tray. For the initial study, manual mixing was used, as well as manual mixing of GPC ingredients like slag or fly ash, fine aggregates, and coarse aggregates [33]. Following the dry mixing of the materials, Figure 5 illustrates how the alkaline activator liquid was added to the dry ingredients of GPC, along with more water, to make the combination more workable. The mixing process was then continued for 4-5 minutes.



Fig. 5. Mixing of Geopolymer concrete.

4.3. Casting and Curing of Specimens

In this study, the concrete specimens are cast to examine the mechanical characteristics of behavior under elevated temperature and essential characteristics such as compression and tension under a controlled state. 216 GPC specimens were cast to test the concrete's mechanical characteristics. The models tested compression strength, splitting stress, and flexural resistance using 72 concrete cubes, cylinders, and prisms. In each group of cubes, 24 models of normal concrete, 24 GPC, and 24 GPC enhanced with steel fibers were tested. Similarly, cylinder and prism tests take place in separate groups.

Furthermore, each group is divided into four various sections. Six models are tested at ambient temperature (0 °C), six models are tested at (250 °C), six models are tested at 500 °C, and the last six models are tested at (750 °C). Before casting, every mold is thoroughly cleaned and lubricated to avoid adhesion with the mixtures. Three layers are used in casting molds. After casting, the top surface of the molds is leveled and smoothed with a trowel, and to stop plastic shrinkage and moisture evaporation from the surface, the specimens are wrapped in nylon sheets for a full day before demolding, as illustrated in Figure 6.



Fig. 6. Casting and curing of specimens.

In this study, Ambient curing is used to compare mechanical qualities. After carefully de-moulding to avoid breaking any edges, the samples are cured with a nylon bag and left at room temperature. Once the specimen has been de-molded, the ambient temperature is recorded throughout the casting. Additionally, the outside temperature is roughly (37–40°C). For 28 days, the specimens are left to dry.

5. Results and Discussion

5.1. Specimens Compression Strength

It is calculated as the percentage difference between the compressive strength after fire exposure and compressive strength at ambient temperature, as shown in Figure 7. The bar chart in (Figure 8) shows the comparative finding of the Compression test of OPC and GPC types and GPC enhanced with steel fiber; the result of the compression test at the ambient curing at the age of 28 days and after exposure to various temperatures shows that all aspects geopolymer and fibrous GPC achieves the highest strength compared to the normal concrete. Findings indicate that all mixes perform differently at fire exposures when exposed to ambient temperatures (AT), 250 °C, 500 °C, and 750 °C.

After comparing the tests, it was found that GPC mixed with steel fibers had the highest compressive strength at the magnitude of (59.46) MPa. It was also illustrated that GPC had a 22% higher compression strength than normal concrete, and fibrous GPC had a 60% higher compression strength than normal concrete because the steel fiber improved the compressive strength.

The findings illustrated that adding steel fiber to GPC increased its splitting tensile strength, as illustrated in other research. The SF has a high bonding strength with the GPC [34], which was higher than the mixes that did not have fiber. The conclusion is that the SF is directly related to the splitting tensile strength of GPC components [35], which reduces cracks in the GPC specimens; thus, the brittle failure is reduced and changes to a ductile failure.

We also found that when the concrete was exposed to various temperatures, its compression strength consistently decreased as the temperature went up. Also, the GPC with steel fibers added had the best compressive strength and resistance to fire at 750 degrees Celsius. The GPC resisted the temperatures and kept its resistance with increasing temperatures.



Fig. 7. The Compressive Strength Test.

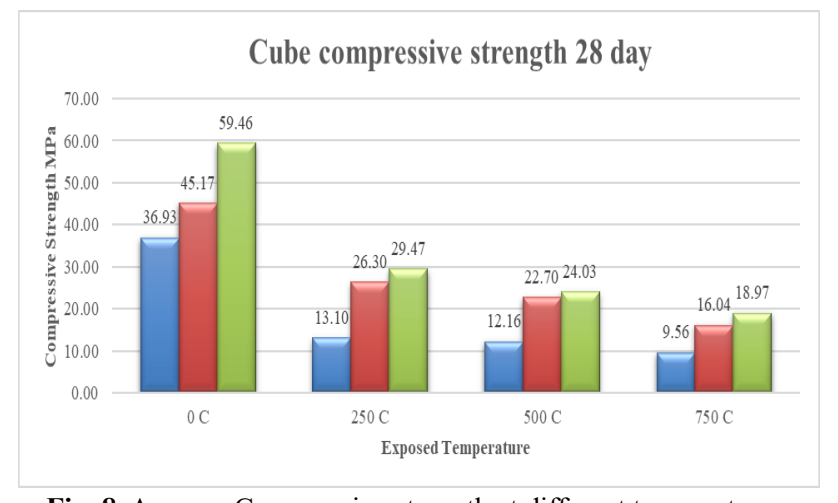


Fig. 8. Average Compressive strength at different temperatures.

No.	Specimen Designation	Cube compressive strength 28 days (MPa)					Average	Standard Deviation	
1	N.C.0	38.5	39.5	37.5	36.4	36.8	32.9	36.93	2.078995
2	N.C.250	15.04	12.69	7.86	11.6	16.86	14.52	13.1	2.880774
3	N.C.500	12.36	10.06	8.94	13.24	14.11	14.27	12.16	2.009947
4	N.C.750	6.42	8.92	9.45	11.41	13.97	7.2	9.56	2.54039
5	G.P.C.0	48.3	45.5	42.5	44.5	46.7	43.5	45.17	1.941363
6	G.P.C.250	17.22	25.84	26.78	31.59	29.76	26.63	26.3	4.526826
7	G.P.C.500	21.87	16.17	28.74	24.92	23.83	20.69	22.7	3.874204
8	G.P.C.750	11.98	10.55	9.07	18.93	20.49	25.2	16.04	5.877425
9	G.P.C (ST.F) 0	60.13	59.3	62.8	58	58.4	58.1	59.46	1.670067
10	G.P.C (ST.F) 250	30.49	23.37	21.51	34.24	33.27	33.94	29.47	5.144346
11	G.P.C (ST.F) 500	14.42	17.77	11.04	30.94	32.55	37.44	24.03	10.00372
12	G.P.C (ST.F) 750	5.03	7.53	8.51	30.14	34.31	28.31	18.97	12.12387

Table 9. Compressive strength at different temperatures.

5.2. Specimens Split Tensile Strength

Figure 9 shows the splitting tensile strength test, while the graph in Figure 10 illustrates the comparative findings of the split tensile test on various types of concrete. The steel fiber GPC demonstrates the highest strength at 3.65 MPa, depending on the split tensile test findings at various temperatures. In comparison, the GGBS and fly ash-based GPC achieve a strength of 2.87 MPa, while normal concrete lags with a lower strength of 1.67 MPa.

It was observed that the geopolymer concrete's maximum split tensile strength decreases as the temperature increases. In all conditions, the steel fiber GPC demonstrates superior resistance, even when exposed to the maximum temperature of 750 °C. At this extreme temperature, the split tensile strength is 1.2 MPa. Table 10 displays each cylinder's findings separately and the average for evaluating six Split tensile strengths under various conditions and temperatures.



Fig. 9. Photo of Split Tensile Strength Test.

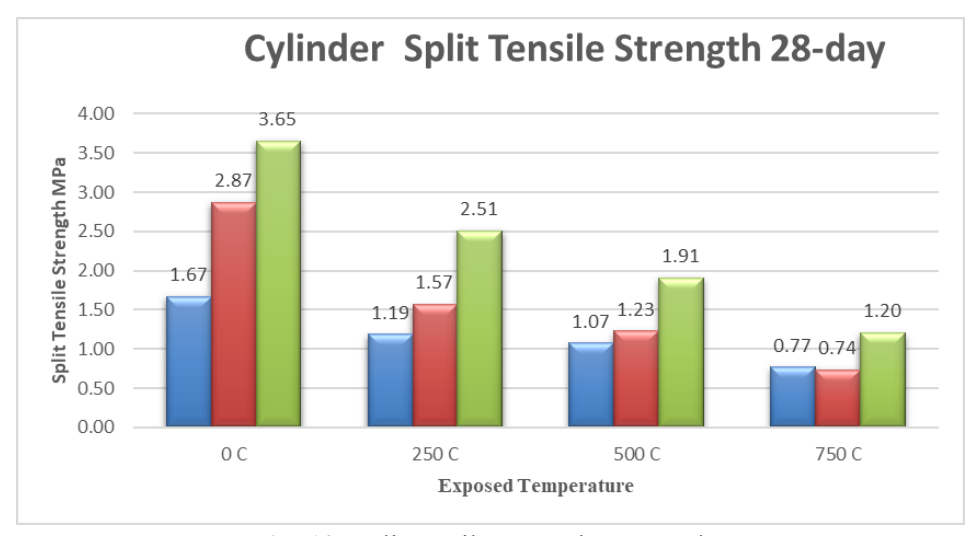


Fig. 10. Split tensile strength test results.

Table 10. Split Tensile strength at different temperatures.

		· · · 1		0			1		
	Model name	C	Cylinder S	plit Tensi	le Streng	th 28-da	y	Average	Standard Deviation
1	N.C.0	1.9	1.48	1.66	1.75	1.66	1.56	1.67	0.133967
2	N.C.250	1.18	1	0.93	1.37	1.42	1.23	1.19	0.178271
3	N.C.500	0.62	0.73	1.14	1.23	1.38	1.34	1.07	0.293693
4	N.C.750	0.59	0.66	0.52	0.71	1.06	1.07	0.77	0.217824
5	G.P.C.0	2.72	3.01	2.8	3.33	2.66	2.7	2.87	0.235089
6	G.P.C.250	1.88	1.62	1.65	1.46	1.48	1.34	1.57	0.17228
7	G.P.C.500	1.09	1.07	1.06	1.4	1.2	1.54	1.23	0.182544
8	G.P.C.750	0.28	0.22	0.25	1.4	1.06	1.22	0.74	0.498411
9	G.P.C (S.F) 0	3.3	3.96	3.64	3.64	3.7	3.67	3.65	0.192217
10	G.P.C (S.F) 250	2.13	1.74	2.77	2.63	3.31	2.48	2.51	0.493322
11	G.P.C (S.F) 500	1.21	1.42	1.43	2.51	2.4	2.48	1.91	0.560578
12	G.P.C (S.F) 750	0.54	1	0.98	1.82	1.56	1.33	1.2	0.419275

5.3. Flexural Strength Test (Modulus of Rupture) (f_r)

The flexural strength test was performed by ASTM C78-15a [36]. The prism specimens were used with dimension $(100x100 \times \times 400)$ mm to identify the flexural strength or Rupture Modulus under a two-point bending load with displacement control. The test was performed at ages 28 and various temperatures, including normal and GPC. Figure 11 shows the flexural strength test.

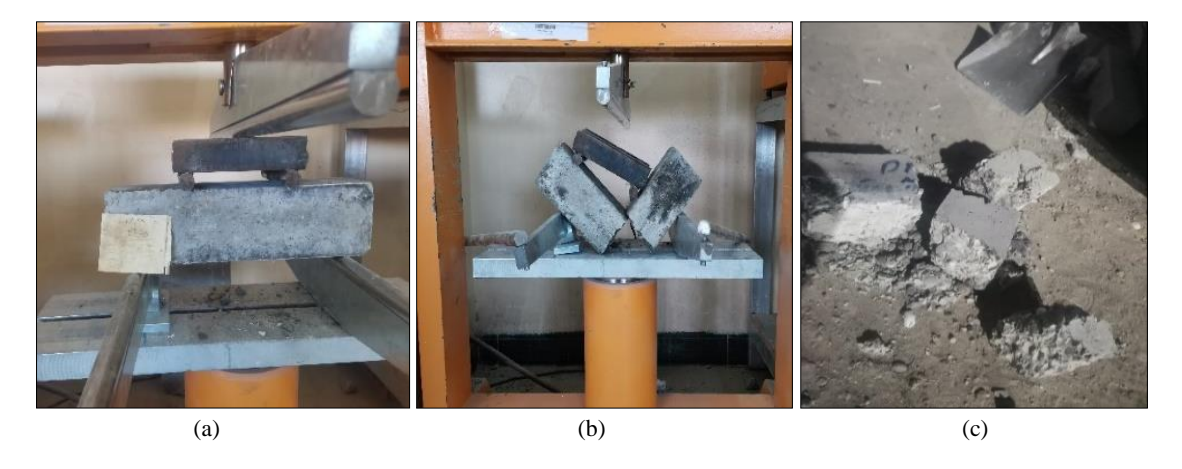


Fig. 11. Flexural strength test machine (Modulus of Rupture Test (f_r)).

The findings of evaluating each prism separately and the average for evaluating six. Flexural strength strengths under various conditions and temperatures are displayed in Table 11. Figure 12 and Table 11 show

that the findings were obtained for regular concrete, geopolymer, and GPC concrete with steel fibers at temperatures (0°C, 250°C, 500°C, and 750°C). It can be seen that the effect of GPC and GPC steel fiber is evident in the bending strength of specimens, which enhances the delayed failure or fracture of the specimen with the appearance of a crack at the bottom of the load, which improves the behavior of specimens after a fracture while reducing its width [37,38].

It should be noted that the models made of ordinary concrete were broken and damaged before the testing process, as illustrated in Figure 12, due to their inability to resist high temperatures, which indicates that in addition to the role played by steel fibers in temperature resistance or due to more bonds between GPC or NC compounds with SF, GPC also works as a thermally insulating and resistant material to high temperatures.

Figure 12 shows that the highest flexural strength magnitude was 6.17 MPa for 0.75% G.P.C (S.F) at ambient curing, 4.90 MPa for GPC, and the lowest magnitude for regular concrete was 4.01 MPa. The flexural resistance decreases with increasing degree of fire. The typical concrete sample had crashed at a temperature of 750°C. In contrast, the GPC and G.P.C (S.F) resisted fire with a magnitude of 1.27 MPa and 1.62 MPa, respectively, at the same temperature. The increase in flexural strength, except for the fibers present, is also due to the high proportion of cementitious materials in the GPC composition [39].

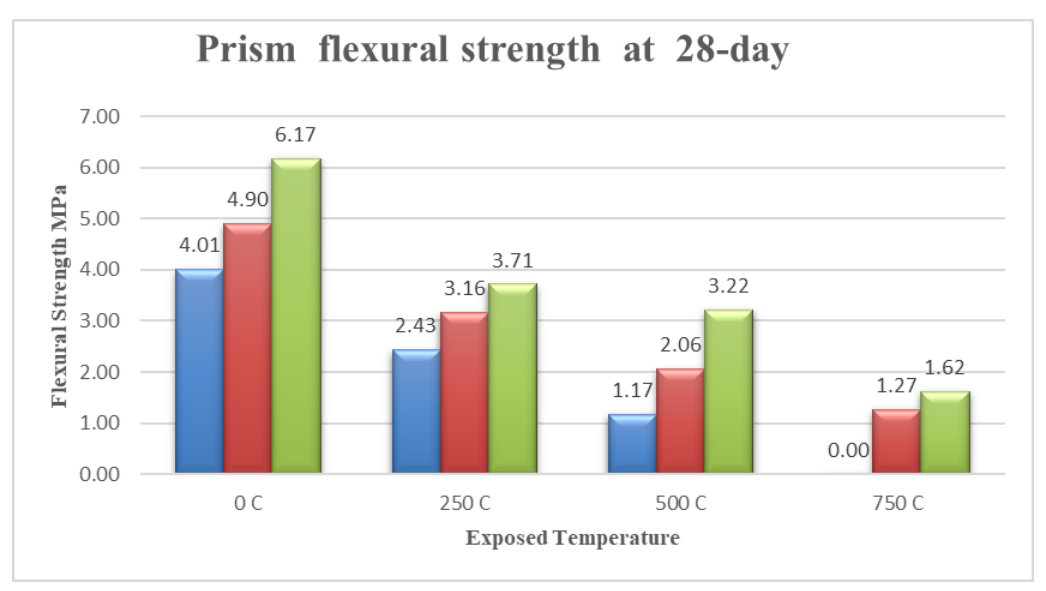


Fig. 12. Flexural strength at different temperatures.

Adding steel fibers to GPC increases its strength primarily due to the reinforcement mechanisms these fibers provide [40,41]. Steel fibers act as crack arresters, bridging micro-cracks in the concrete matrix and distributing applied stresses more evenly throughout the material [42] to prevent the formation and propagation of larger cracks, which delays the onset of failure and enhances the overall toughness and ductility of the concrete. In compressive loading, the steel fibers help confine the concrete, improving its load-bearing capacity by resisting internal tensile stresses that develop during compression [43,44]. In tensile and flexural applications, the fibers significantly improve the material's ability to resist bending and stretching, as they help to carry tensile loads across cracks that would otherwise cause brittle failure in conventional concrete [45,46]. Additionally, steel fibers enhance the bonding within the concrete matrix, especially in high-temperature conditions, by maintaining structural integrity and reducing the likelihood of catastrophic failure [47,48]. This increased ductility and toughness provided by steel fibers are crucial for improving the durability and resilience of GPC, particularly under fire exposure or dynamic loading conditions.

	Model name		Prism	flexural st	trength at	28-day		Average	Standard Deviation
1	N.C.0	4.36	4.44	4.2	4.16	3.48	3.4	4.01	0.412095
2	N.C.250	1.948	1.1	1.42	3.32	3.46	3.332	2.43	0.973647
3	N.C.500	1.84	0.816	1.18	1.06	1.18	0.932	1.17	0.327398
4	N.C.750	0	0	0	0	0	0	0	0
5	G.P.C.0	5.72	5	5.32	4.56	4.32	4.48	4.9	0.497862
6	G.P.C.250	2.824	3.58	4.848	2.52	2.58	2.62	3.16	0.834288
7	G.P.C.500	1.428	1.736	1.78	2.56	2.32	2.532	2.06	0.432663
8	G.P.C.750	0.728	0.642	0.78	2.04	1.68	1.744	1.27	0.564789
9	G.P.C (S.F) 0	7.44	7.56	7.4	4.74	5.024	4.86	6.17	1.299501
10	G.P.C (S.F) 250	4.496	3.42	3.952	3.3	3.7	3.42	3.71	0.410818
11	G.P.C (S.F) 500	3.22	3.064	3.156	2.924	3.656	3.3	3.22	0.228234
12	G.P.C (S.F) 750	1.484	0.928	1.02	2.172	1.832	2.26	1.62	0.519056

Table 11. Flexural strength at different temperatures.

5.4. Mathematical Modeling

In this part, two equations have been used to evaluate the estimated values of both splitting tensile strength and Flexural strength based on ACI code:

$$f_t = 0.56 \times \sqrt{f_c} \tag{1}$$

$$f_r = 0.62 \times \sqrt{f_c} \tag{2}$$

Figure 13 shows the relationship between the estimated splitting tensile strength from ACI 318 code and the obtained results from experimental work. The coefficient of determination, $R^2=0.8337$, demonstrates approximately 83.4% with good fitting.

Figure 14 shows the relationship between the estimated flexural strength from the ACI 318 code and the results obtained from experimental work. The coefficient of determination, R^2 =0.9178, implies that the obtained values explain 91.8% of the variability in estimated flexural strength, suggesting a highly accurate estimation model with minimal variability.

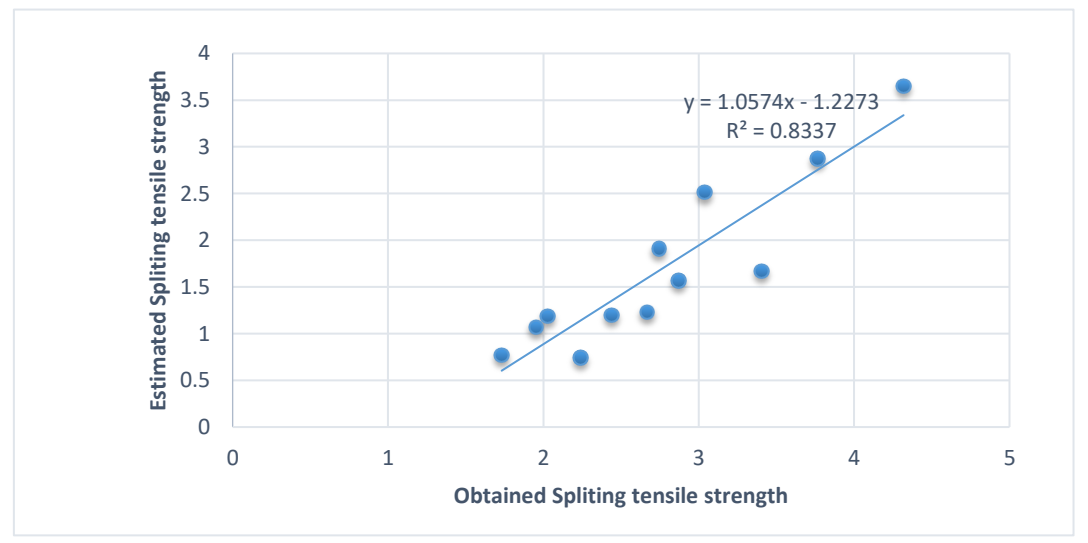


Fig. 13. The relationship between estimated splitting tensile strength based on ACI code equation and experimental results.

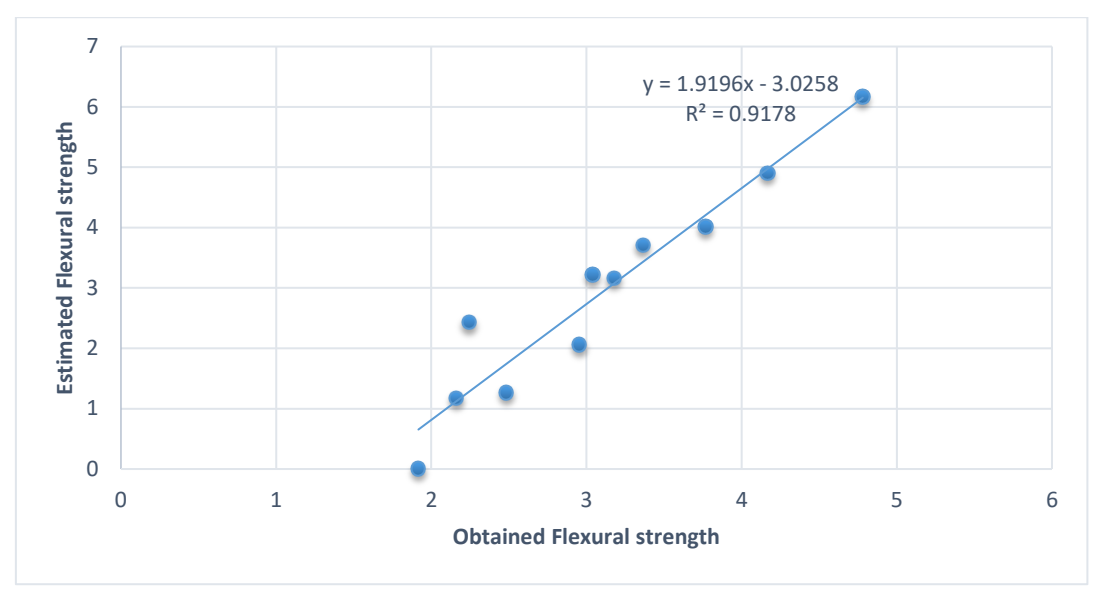


Fig. 14. The relationship between estimated flexural strength based on ACI code equation and experimental results.

5.5. Scanning Electron Microscopy (SEM)

The SEM images presented in Figure 15 provide essential insights into the microstructural changes in geopolymer pastes containing varying percentages of ground granulated blast furnace slag (GGBS) as substitutes for fly ash (FA) at different temperatures (0, 250, 500, and 750°C). The compact and nearly fully reacted microstructure observed in the SEM images indicates a well-developed geopolymer matrix at elevated temperatures. The presence of unreacted FA particles, such as cenospheres and planispheres, suggests that these particles, while not acting as fillers initially, may contribute to the long-term strengthening of the matrix by facilitating gradual reactions over time [49].

The SEM images reveal geopolymerization products such as calcium-silicate-hydrate (C-S-H) and alumina-silicate-hydrate (A-S-H) gels, mainly when 20% GGBS is activated in the presence of FA. These gels are crucial to enhancing the material's strength, as they contribute to the densification of the matrix. The interaction between the calcium from GGBS and the alumina-silicate from FA forms calcium alumina-silicate hydrate (C-A-S-H), further reinforcing the matrix and improving mechanical properties and thermal stability at higher temperatures. The densified matrix enhances durability by reducing porosity and improving thermal degradation resistance [50,51].

Additionally, the SEM analysis shows the formation of Na-Al(Mg)-Si-H gel, likely influenced by the Mg²⁺ from GGBS [52]. This new gel phase plays a significant role in further strengthening the geopolymer network, enhancing its setting characteristics and overall mechanical performance. The micro-cracks observed in the SEM images are likely artifacts from mechanical testing caused by internal stress during the microstructure formation or by the mechanical tests conducted prior to SEM sample preparation. The formation of needle-like structures on the surface of FA particles suggests the influence of high concentrations of the alkaline activator solution, which partially reacted and formed micro-needle particles during the polymerization process. These structures could influence the material's mechanical behavior, potentially acting as stress concentrators in certain conditions [53]. Overall, the densification of the geopolymer matrix at 500°C and 750°C appears to produce the most homogeneous and robust structure. At the same time, the microstructure at 0°C shows a lack of homogeneity, possibly due to incomplete reactions or lower levels of polymerization [54], which indicates that elevated temperatures are critical in optimizing geopolymer concrete's mechanical properties and durability, as the improved microstructure at higher temperatures results in better performance.

Using Fly Ash and GGBS in GPC enhances both performance and sustainability. Fly ash contributes to strength by filling voids, creating a denser matrix, and reducing the heat of hydration, minimizing the risk of thermal cracking. GGBS adds calcium ions that form calcium-silicate-hydrate (C-S-H) and calcium-alumina-silicate-hydrate (C-A-S-H) gels, further boosting strength and durability. Fly ash and GGBS improve resistance to sulfate attacks, thermal stability, and chemical durability, making GPC an environmentally friendly, durable alternative to traditional cement, ideal for high-temperature and aggressive environments.

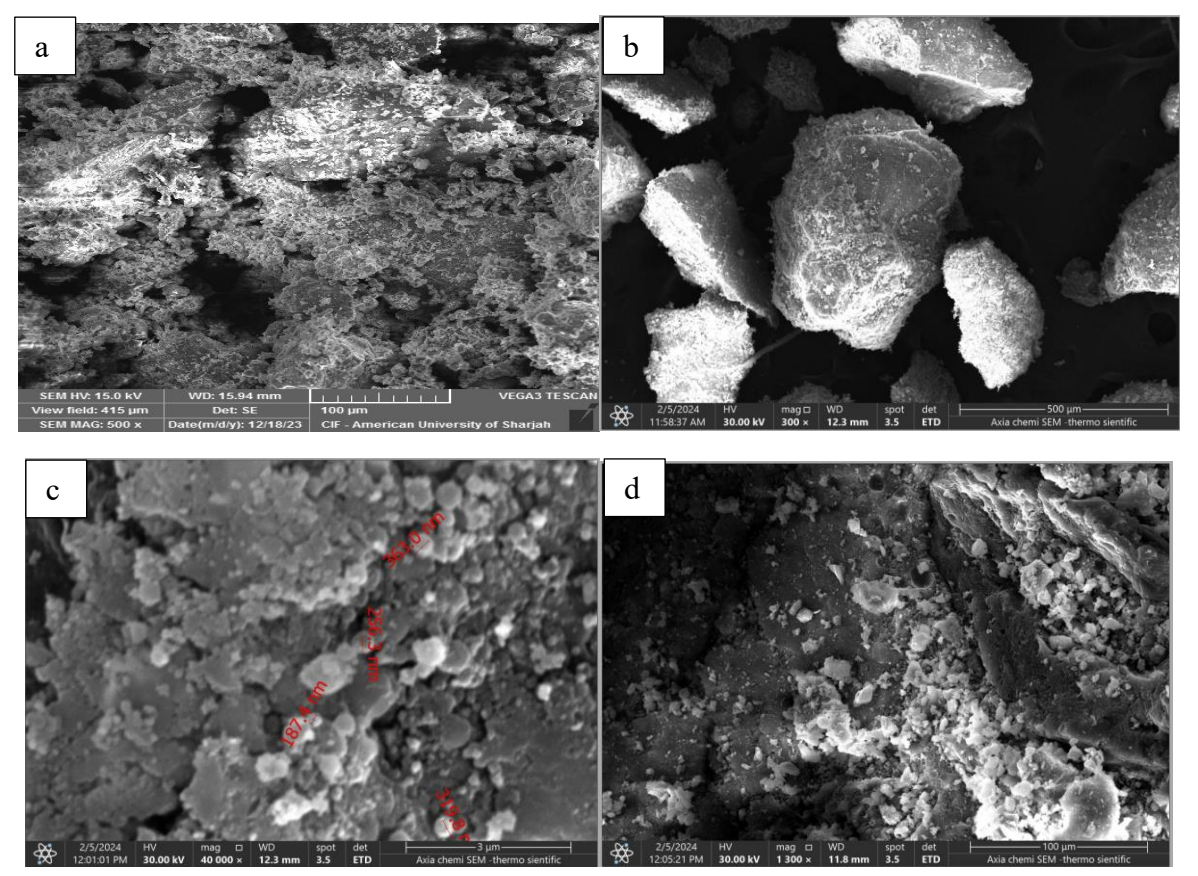


Fig. 15. SEM images for Geopolymer concrete subject to various temperatures: a) at 0oC; b) at 250oC; c) at 500oC; d) at 750oC.

Conclusion

- The study shows that GPC is more effective and retains strength better than normal concrete when exposed to high temperatures due to geopolymers' lower thermal nontraditional cementitious materials, which provide insulation. Additionally, increased concrete temperature reduces confined compressive strength in all cases.
- The compressive strength of GPC increased by 22.3% compared to normal concrete, while GPC enhanced with steel fiber showed a 61% increase. Similarly, the split tensile strength of GPC rose by 71.8%, with the steel fiber-enhanced version achieving a 118.5% increase over normal concrete.
- Regarding flexural strength, GPC demonstrated a 22% increase in rupture strength compared to normal concrete, while the steel fiber-enhanced GPC exhibited a 54% increase.
- Based on the experimental findings, including steel fiber significantly impacts mechanical strength. The optimal steel fiber proportion of 0.75% improves all mechanical properties, preserving strength to the greatest extent.

• While adding steel fiber reduces workability, making GPC more challenging to handle than regular concrete, it significantly enhances the mechanical properties. It increases the concrete's durability, particularly in terms of fire resistance.

Future work should incorporate mathematical modeling to predict compressive, tensile, and flexural strength reductions under elevated temperatures, mainly using degradation models and finite element analysis. This approach would enhance understanding of GPC and GPC-SF performance, enabling more precise design for high-temperature applications and fire resistance.

Acknowledgments

Tikrit University supported this work.

Funding

This research received no specific grant from funding agencies in the public, commercial, or not-for-profit sectors.

Conflicts of interest

The authors declare that they have no known competing financial interests or personal relationships that could have appeared to influence the work reported in this paper.

The author is an Editorial Board Member/Editor-in-Chief/Associate Editor/Guest Editor for [Journal name] and was not involved in the editorial review or the decision to publish this article.

The authors declare the following financial interests/personal relationships which may be considered as potential competing interests.

Authors contribution statement

Arjan Abdullah: Methodology; Writing – original draft.

Mazin Abdul-Rahman: Supervision; Writing – review & editing.

Alyaa Al-Attar: Supervision; Writing – review & editing.

References

- [1] Marshdi QSR, Hussien SA, Mareai BM, Al-Khafaji ZS, Shubbar AA. Applying of No-fines concretes as a porous concrete in different construction application. Period Eng Nat Sci 2021;9:999–1012. https://doi.org/10.21533/pen.v9i4.2476.
- [2] Majdi HS, Shubbar AA, Nasr MS, Al-Khafaji ZS, Jafer H, Abdulredha M, et al. Experimental data on compressive strength and ultrasonic pulse velocity properties of sustainable mortar made with high content of GGBFS and CKD combinations. Data Br 2020;31:105961.
- [3] Kadhim S, Shubbar A, Al-Khafaji Z, Nasr M, Al-Mamoori S, Falah MW. Development of ternary blend cement-free binder material for construction. Eur J Environ Civ Eng 2024:1–14. https://doi.org/10.1080/19648189.2024.2326977.
- [4] Shubbar AA, Jafer H, Abdulredha M, Al-Khafaji ZS, Nasr MS, Al Masoodi Z, et al. Properties of cement mortar incorporated high volume fraction of GGBFS and CKD from 1 day to 550 days. J Build Eng 2020;30:101327. https://doi.org/10.1016/j.jobe.2020.101327.

- [5] Falah MW, Hafedh AA, Hussein SA, Al-Khafaji ZS, Shubbar AA, Nasr MS. The Combined Effect of CKD and Silica Fume on the Mechanical and Durability Performance of Cement Mortar. Key Eng. Mater., vol. 895, Trans Tech Publ; 2021, p. 59–67.
- [6] Hamad MA, Nasr M, Shubbar A, Al-Khafaji Z, Al Masoodi Z, Al-Hashimi O, et al. Production of Ultra-High-Performance Concrete with Low Energy Consumption and Carbon Footprint Using Supplementary Cementitious Materials Instead of Silica Fume: A Review. Energies 2021;14:8291. https://doi.org/10.3390/en14248291.
- [7] Humad AM, Dakhil AJ, Al-Mashhadi SA, Al-Khafaji Z, Mohammed ZA, Jabr SF. Improvements of mechanical and physical features of cement mortar by nano AL2O3 and CaCO3 as additives. Res Eng Struct Mater 2024;10. https://doi.org/10.17515/resm2023.43me0806rs.
- [8] Al-Khafaji ZS, Al Masoodi Z, Jafer H, Dulaimi A, Atherton W. The Effect Of Using Fluid Catalytic Cracking Catalyst Residue (FC3R)" As A Cement Replacement In Soft Soil Stabilisation. Int J Civ Eng Technol Vol 2018;9:522–33.
- [9] Makul N. Advanced smart concrete-A review of current progress, benefits and challenges. J Clean Prod 2020;274:122899.
- [10] Kibert CJ. Sustainable construction: green building design and delivery. John Wiley & Sons; 2016.
- [11] Imbabi MS, Carrigan C, McKenna S. Trends and developments in green cement and concrete technology. Int J Sustain Built Environ 2012;1:194–216.
- [12] Harrison T, Jones MR, Lawrence D. The production of low energy cements. Lea's Chem Cem Concr 2019:341–61.
- [13] Gartner E. Industrially interesting approaches to "low-CO2" cements. Cem Concr Res 2004;34:1489–98. https://doi.org/10.1016/j.cemconres.2004.01.021.
- [14] Nuaklong P, Jongvivatsakul P, Pothisiri T, Sata V, Chindaprasirt P. Influence of rice husk ash on mechanical properties and fire resistance of recycled aggregate high-calcium fly ash geopolymer concrete. J Clean Prod 2020;252:119797.
- [15] Lahoti M, Tan KH, Yang E-H. A critical review of geopolymer properties for structural fire-resistance applications. Constr Build Mater 2019;221:514–26.
- [16] Zeini HA, Al-jeznawi D, Imran H, Filipe L, Bernardo A, Al-khafaji Z, et al. Random Forest Algorithm for the Strength Prediction of Geopolymer Stabilized Clayey Soil 2023:1–15. https://doi.org/10.3390/su15021408.
- [17] AL-JABERI LA, Ali A, Al-Jadiri RS, Al-Khafaji Z. Workability and Compressive Strength Properties of (Fly Ash-Metakaolin) based Flowable Geopolymer Mortar. Electron J Struct Eng 2023;23:46–51. https://doi.org/10.56748/ejse.23436.
- [18] Al-Husseinawi FN, Atherton W, Al-Khafaji Z, Sadique M, Yaseen ZM. The Impact of Molar Proportion of Sodium Hydroxide and Water Amount on the Compressive Strength of Slag/Metakaolin (Waste Materials) Geopolymer Mortar. Adv Civ Eng 2022;2022. https://doi.org/10.1155/2022/5910701.
- [19] Oyebisi S, Akinmusuru J, Ede A, Ofuyatan O, Mark G, Oluwafemi J. 14 molar concentrations of alkaliactivated geopolymer concrete. IOP Conf. Ser. Mater. Sci. Eng., vol. 413, IOP Publishing; 2018, p. 12065.
- [20] Amran M, Huang S-S, Debbarma S, Rashid RSM. Fire resistance of geopolymer concrete: A critical review. Constr Build Mater 2022;324:126722.
- [21] Zhang H, Sarker PK, Wang Q, He B, Kuri JC, Jiang Z. Comparison of compressive, flexural, and temperature-induced ductility behaviours of steel-PVA hybrid fibre reinforced OPC and geopolymer concretes after high temperatures exposure. Constr Build Mater 2023;399:132560.
- [22] Abd Razak SN, Shafiq N, Guillaumat L, Wahab MMA, Farhan SA, Husna N, et al. Fire performance of fly ash-based geopolymer concrete: Effect of burning temperature. IOP Conf. Ser. Earth Environ. Sci., vol. 945, IOP Publishing; 2021, p. 12062.
- [23] Ekinci E, Türkmen İ, Kantarci F, Karakoç MB. The improvement of mechanical, physical and durability characteristics of volcanic tuff based geopolymer concrete by using nano silica, micro silica and Styrene-Butadiene Latex additives at different ratios. Constr Build Mater 2019;201:257–67.
- [24] Yazdi MA, Liebscher M, Hempel S, Yang J, Mechtcherine V. Correlation of microstructural and mechanical properties of geopolymers produced from fly ash and slag at room temperature. Constr Build Mater 2018;191:330–41.

- [25] He R, Dai N, Wang Z. Thermal and mechanical properties of geopolymers exposed to high temperature: a literature review. Adv Civ Eng 2020;2020:7532703.
- [26] Korniejenko K, Frączek E, Pytlak E, Adamski M. Mechanical properties of geopolymer composites reinforced with natural fibers. Procedia Eng 2016;151:388–93.
- [27] Cheng Z, He L, Wang L, Liu Y, Yang S, He Z, et al. Effect of textile sludge on strength, shrinkage, and microstructure of polypropylene fiber concrete. Buildings 2023;13:379.
- [28] Zhang HY, Kodur V, Wu B, Cao L, Wang F. Thermal behavior and mechanical properties of geopolymer mortar after exposure to elevated temperatures. Constr Build Mater 2016;109:17–24.
- [29] Sarker PK, Mcbeath S. Fire endurance of steel reinforced fly ash geopolymer concrete elements. Constr Build Mater 2015;90:91–8.
- [30] IQS-5. Iraqi Standard Specification for the Portland Cement. Cent Organ Stand Qual Control Baghdad, Iraq 2005.
- [31] Sujatha T, Kannapiran K, Nagan S. Strength assessment of heat cured geopolymer concrete slender column. ASIAN J Civ Eng (BUILDING HOUSING) 2012;13:635–46.
- [32] ME CR, Rao AB. Behavior of self compacting concrete under axial compression with and without confinement. Int J Ethics Eng Manag Educ 2014;1.
- [33] Vijai K, Kumutha R, Vishnuram BG. Effect of types of curing on strength of geopolymer concrete. Int J Phys Sci 2010;5:1419–23.
- [34] Shaikh FUA. Pullout behavior of hook end steel fibers in geopolymers. J Mater Civ Eng 2019;31:4019068.
- [35] Athiyamaan V, Ganesh GM. Experimental, statistical and simulation analysis on impact of micro steel—Fibres in reinforced SCC containing admixtures. Constr Build Mater 2020;246:118450.
- [36] Standard A. C78. 2002. Standard test method for flexural strength of concrete (using simple beam with third point loading). Annu B ASTM Stand 2002;4.
- [37] Mo KH, Yeoh KH, Bashar II, Alengaram UJ, Jumaat MZ. Shear behaviour and mechanical properties of steel fiber-reinforced cement-based and geopolymer oil palm shell lightweight aggregate concrete. Constr Build Mater 2017;148:369–75.
- [38] Khan MZN, Hao Y, Hao H, Shaikh FUA. Mechanical properties of ambient cured high strength hybrid steel and synthetic fibers reinforced geopolymer composites. Cem Concr Compos 2018;85:133–52.
- [39] Nath P, Sarker PK. Flexural strength and elastic modulus of ambient-cured blended low-calcium fly ash geopolymer concrete. Constr Build Mater 2017;130:22–31.
- [40] Tran TT, Pham TM, Hao H. Experimental and analytical investigation on flexural behaviour of ambient cured geopolymer concrete beams reinforced with steel fibers. Eng Struct 2019;200:109707.
- [41] Abdullah M, Tahir MFM, Tajudin M, Ekaputri JJ, Bayuaji R, Khatim NAM. Study on the geopolymer concrete properties reinforced with hooked steel fiber. IOP Conf. Ser. Mater. Sci. Eng., vol. 267, IOP Publishing; 2017, p. 12014.
- [42] Ponnambalam N, Thangavel S, Murali G, Vatin NI. Impact strength of preplaced aggregate concrete comprising glass fibre mesh and steel fibres: experiments and modeling. Materials (Basel) 2022;15:5259.
- [43] Xiang Z, Zhou J, Niu J. Compressive behavior of CFRP-confined steel fiber-reinforced self-compacting lightweight aggregate concrete in square columns. J Build Eng 2022;59:105118.
- [44] Li H, Li X, Fu J, Zhu N, Chen D, Wang Y, et al. Experimental study on compressive behavior and failure characteristics of imitation steel fiber concrete under uniaxial load. Constr Build Mater 2023;399:132599.
- [45] Ahmad J, Burduhos-Nergis DD, Arbili MM, Alogla SM, Majdi A, Deifalla AF. A review on failure modes and cracking behaviors of polypropylene fibers reinforced concrete. Buildings 2022;12:1951.
- [46] Ahmad J, González-Lezcano RA, Majdi A, Ben Kahla N, Deifalla AF, El-Shorbagy MA. Glass fibers reinforced concrete: Overview on mechanical, durability and microstructure analysis. Materials (Basel) 2022;15:5111.
- [47] Zhou A, Qiu Q, Chow CL, Lau D. Interfacial performance of aramid, basalt and carbon fiber reinforced polymer bonded concrete exposed to high temperature. Compos Part A Appl Sci Manuf 2020;131:105802.
- [48] Hamidi F, Carré H, Hamami AEA, Aït-Mokhtar A, La Borderie C, Pimienta P. Critical review of the use of fiber-reinforced concrete against spalling. Fire Saf J 2023:103988.

- [49] Ryu GS, Lee YB, Koh KT, Chung YS. The mechanical properties of fly ash-based geopolymer concrete with alkaline activators. Constr Build Mater 2013;47:409–18.
- [50] Kumar S, Kumar R, Mehrotra SP. Influence of granulated blast furnace slag on fly ash-based geopolymer's reaction, structure and properties. J Mater Sci 2010;45:607–15.
- [51] Nath SK, Kumar S. Influence of iron making slags on strength and microstructure of fly ash geopolymer. Constr Build Mater 2013;38:924–30.
- [52] Nath P, Sarker PK. Effect of GGBFS on setting, workability and early strength properties of fly ash geopolymer concrete cured in ambient condition. Constr Build Mater 2014;66:163–71.
- [53] Fernández-Jiménez A, García-Lodeiro I, Palomo A. Durability of alkali-activated fly ash cementitious materials. J Mater Sci 2007;42:3055–65.
- [54] Alehyen S, Achouri MEL, Taibi M. Characterization, microstructure and properties of fly ash-based geopolymer. J Mater Environ Sci 2017;8:1783–96.